INFECTION AND IMMUNITY, Nov. 2007, p. 5376–5389 Vol. 75, No. 11
0019-9567/07/$08.00+0 doi:10.1128/IAI.00238-07

Identification of *Francisella tularensis Himar1*-Based Transposon Mutants Defective for Replication in Macrophages[▽]

Tamara M. Maier,[1] Monika S. Casey,[1] Rachel H. Becker,[1] Caleb W. Dorsey,[1] Elizabeth M. Glass,[2] Natalia Maltsev,[2] Thomas C. Zahrt,[1] and Dara W. Frank[1]*

Department of Microbiology and Molecular Genetics, Medical College of Wisconsin, 8701 Watertown Plank Road, Milwaukee, Wisconsin 53226,[1] and Mathematics and Computer Science Division of the Computational Biology Group, Argonne National Laboratory, 9700 S. Cass Avenue, Argonne, Illinois 60439[2]

Received 13 February 2007/Returned for modification 26 March 2007/Accepted 26 July 2007

***Francisella tularensis*, the etiologic agent of tularemia in humans, is a potential biological threat due to its low infectious dose and multiple routes of entry. *F. tularensis* replicates within several cell types, eventually causing cell death by inducing apoptosis. In this study, a modified *Himar1* transposon (*HimarFT*) was used to mutagenize *F. tularensis* LVS. Approximately 7,000 Km^r clones were screened using J774A.1 macrophages for reduction in cytopathogenicity based on retention of the cell monolayer. A total of 441 candidates with significant host cell retention compared to the parent were identified following screening in a high-throughput format. Retesting at a defined multiplicity of infection followed by in vitro growth analyses resulted in identification of approximately 70 candidates representing 26 unique loci involved in macrophage replication and/or cytotoxicity. Mutants carrying insertions in seven hypothetical genes were screened in a mouse model of infection, and all strains tested appeared to be attenuated, which validated the initial in vitro results obtained with cultured macrophages. Complementation and reverse transcription-PCR experiments suggested that the expression of genes adjacent to the *HimarFT* insertion may be affected depending on the orientation of the constitutive *groEL* promoter region used to ensure transcription of the selective marker in the transposon. A hypothetical gene, FTL_0706, postulated to be important for lipopolysaccharide biosynthesis, was confirmed to be a gene involved in O-antigen expression in *F. tularensis* LVS and Schu S4. These and other studies demonstrate that therapeutic targets, vaccine candidates, or virulence-related genes may be discovered utilizing classical genetic approaches in *Francisella*.**

Francisella tularensis is a gram-negative intracellular pathogen and the etiologic agent of human tularemia. The CDC has classified *F. tularensis* as a category A select agent due to its highly infectious nature and ease of dissemination. Four subspecies of *F. tularensis* have been recognized, including (i) the virulent type A *F. tularensis* subsp. *tularensis*, (ii) the less virulent type B *F. tularensis* subsp. *holarctica*, (iii) *F. tularensis* subsp. *mediasiatica*, and (iv) *F. tularensis* subsp. *novicida*. The *F. tularensis* LVS (live vaccine strain) is derived from *F. tularensis* subsp. *holarctica* and is used as a model system to identify *Francisella* virulence factors since it is attenuated in humans but virulent in mice (8, 21). The limited genetic variation (2 to 4%) between the subspecies of *Francisella* suggests that there is potential overlap among genes related to pathogenesis (7, 54, 59). In fact, *F. tularensis* LVS and Schu S4 vary in genomic sequence by less than 1% (59). Regardless of the high sequence similarity at the genomic level, genome rearrangement and variation at the functional or regulatory level among the subspecies clearly result in phenotypes that impact virulence and pathogenesis (12, 15, 29, 54, 73, 74).

The life cycle of *F. tularensis* inside the macrophage begins with surface receptor binding and entry into a vacuole involving pseudopod loops, subsequent escape into the cytoplasm, where replication occurs, and release from the macrophage through apoptosis (for reviews, see references 44, 51, and 65). A role for autophagy after cytoplasmic replication has been described recently (11). *Francisella* can replicate intracellularly in macrophages, hepatocytes, endothelial cells, epithelial cells, fibroblasts, chicken embryos, and amoebae (for reviews, see references 19, 51, and 71). The fact that *Francisella* can thrive in such diverse environments suggests that a variety of virulence genes are required to facilitate its survival.

An initial barrier to using gene modification approaches to identify potential virulence factors in *Francisella* was the lack of genetic tools. Recent advances, however, have overcome this limitation with the development of shuttle plasmids (6, 40, 41, 57), transposons (23, 33, 42), and allelic replacement strategies (27, 36). The genes predicted to foster intracellular growth and virulence include the genes in operons encoding *iglABCD* and *pdpABCD* proteins present on the *Francisella* pathogenicity island (FPI), as well as genes involved in oxidative stress or protein turnover, capsule or lipopolysaccharide (LPS) biosynthesis, type IV pilin assembly, iron uptake, outer membrane channels, purine biosynthesis, and regulation through *mglAB* or *pmrA* (44, 46, 50, 51, 53, 56, 65, 66). Although information on the *Francisella* life cycle, *Francisella* intracellular growth, and several target virulence factors has been obtained, little is known about the mechanisms involved in pathogenesis in different subspecies and environmental niches. Genomic annotations for *Francisella* indicate that up to 30% of the open reading frames encode hypothetical proteins (23, 35, 54) which have the potential to function as novel virulence factors.

* Corresponding author. Mailing address: Department of Microbiology and Molecular Genetics, Medical College of Wisconsin, 8701 Watertown Plank Road, Milwaukee, WI 53226. Phone: (414) 955-8766. Fax: (414) 955-6567. E-mail: frankd@mcw.edu.

▽ Published ahead of print on 6 August 2007.

TABLE 1. Bacterial strains, plasmids and primers used in this study

Strain, plasmid, or primer	Description	Reference(s) and/or source
F. tularensis strains		
LVS	*F. tularensis* subsp. *holartica* live vaccine strain; type B	18; K. L. Elkins
U112	*F. tularensis* subsp. *novicida* type B strain (isolated from water in Utah, 1950)	34
Schu S4	*F. tularensis* subsp. *tularensis* type A strain (isolated from a human ulcer in Ohio, 1941)	17; BEI Resources
TCZ1013	LVS Δ*purMCD*::*groE-aph*	53
LVS FTL_0741::*HimarFT*	LVS *HimarFT* mutant strain with an insertion in the hypothetical gene FTL_0741 used as a *HimarFT*-containing control strain displaying a wild-type phenotype in our in vitro and in vivo analyses	This study
LVS FTL_0706-1::*HimarFT*	LVS *HimarFT* mutant with an insertion in FTL_0706 with the *groEL* promoter (p*gro*) from *HimarFT* in the same orientation as FTL_0706	This study
LVS FTL_0706-2::*HimarFT*	LVS *HimarFT* mutant with an insertion in FTL_0706 with the *groEL* promoter (p*gro*) from *HimarFT* in the orientation opposite that of FTL_0706	This study
LVS *wbtA1*::*HimarFT*	LVS *HimarFT* mutant with an insertion in *wbtA* with the *groEL* promoter (p*gro*) from *HimarFT* in the orientation opposite that of *wbtA*	This study
LVS *wbtA2*::*HimarFT*	LVS *HimarFT* mutant with an insertion in *wbtA* with the *groEL* promoter (p*gro*) from *HimarFT* in the same orientation as *wbtA*	This study
LVS *wbtM*::*HimarFT*	LVS *HimarFT* mutant with an insertion in *wbtM* with the *groEL* promoter (p*gro*) from *HimarFT* in the same orientation as *wbtM*	This study
LVS *wbtC*::*HimarFT*	LVS *HimarFT* mutant with an insertion in *wbtC* with the *groEL* promoter (p*gro*) from *HimarFT* in the same orientation as *wbtC*	This study
Schu S4 FTT1238c::*HimarFT* (meriodipoid)	Schu S4 FTT1238c::*HimarFT* resulting from homologous recombination with SpeI circularized genomic DNA from LVS producing a single crossover in the Schu S4 genome	This study
Schu S4 FTT1238c::*HimarFT*	Schu S4 FTT1238c::*HimarFT* resulting from homologous recombination with SpeI circularized genomic DNA from LVS producing a double crossover in the Schu S4 genome	This study
E. coli strains		
DH5α	F$^-$ ϕ80*lacZ*Δ*M15 endA1 recA1 hsdR17 supE44 thi-1 gyrA96 relA1* Δ(*lacZYA–argF*)*U169*	Invitrogen
DH5αλpir	As DH5α, lysogenized with λpir phage; used as host for *HimarFT* rescue	A. Camilli
TOP10	F$^-$ *mcrA* Δ(*mrr-hsdRMS-mcrBC*) ϕ80*lacZ*Δ*M15* Δ*lacX74 deoR recA1 araD139* Δ(*ara-leu*)*7697 galU galK rpsL*(Sm^r) *endA1 nupG*; used as host for plasmids derived from pCR2.1-TOPO	Invitrogen
Plasmids[a]		
pCR2.1-TOPO	3.9-kb plasmid for cloning PCR products; Km^r Ap^r	Invitrogen
pCR-Blunt II-TOPO	3.5-kb plasmid for cloning PCR products; Km^r	Invitrogen
pAG36	6.1-kb plasmid used as the source of the nourseothricin resistance marker; Ap^r Nt^r	Euroscarf
pFNLTP7	6.9-kb pFNLTP1 derivative with XhoI, StuI, PacI, SpeI, HpaI, and NdeI restriction enzyme sites (MCS3) cloned between the KpnI and BamHI sites; Km^r Ap^r	41
pFNLTP16 H3	10-kb derivative of pFNLTP16 containing *HimarFT* (*Himar1* modified with the *F. tularensis* LVS *groEL* promoter in the BclI site upstream of *aphA-2*); Km^r Ap^r	42
pHimar H3	4.3-kb plasmid containing *HimarFT* and a minimal suicide vehicle containing the essential *tnp* for transposition; Km^r	This study
pFTNAT	6.3-kb derivative of pFNLTP7 lacking kanamycin and ampicillin resistance and containing nourseothricin acetyltransferase flanked with NotI; Nt^r	This study
pFTNAT-$wbtA_{LVS}$	8.7-kb plasmid containing *wbtA* and 472-bp upstream sequence used for complementation; Nt^r	This study
pFTNAT-$wbtM_{LVS}$	8.0-kb plasmid containing *wbtM* and 481-bp upstream sequence used for complementation; Nt^r	This study
pFTNAT-FTL_0706	8.0-kb plasmid containing FTL_0706 and 175-bp upstream sequence used for complementation; Nt^r	This study
Primers[b]		
C1	5′-TGAGTAGCTATATTGGTAACTC-3′; forward primer for *wbtC* for RT-PCR of 366-bp fragment	
C2	5′-TCAGTTTGAAGCTTACTATCTC-3′; reverse primer for *wbtC* for RT-PCR of 366-bp fragment	
D1	5′-TGAATTGTTAGAAGCCTTTGC-3′; forward primer for *wbtD* for RT-PCR of 410-bp fragment	
D2	5′-TTAGCTCTAGCTTTATAGCTC-3′; reverse primer for *wbtD* for RT-PCR of 410-bp fragment	
H1	5′-CTAAAGTAGTTTTACTAGCAGC-3′; forward primer for 423-bp N-terminal FTL_0706 probe	

Continued on following page

TABLE 1—*Continued*

Strain, plasmid, or primer	Description	Reference(s) and/or source
H2	5′-TCACTTATTATAAAATAATCTCCC-3′; reverse primer for 423-bp N-terminal FTL_0706 probe	
H3	5′-CGGGATCCAAAATGTAGAGTAGGAATGGGT; forward primer for 2-kb FTL_0706 fragment for complementation	
H4	5′-CCGCTCGAGGGATAATGAGTTGTTAGATGCT-3′; reverse primer for 2-kb FTL_0706 fragment for complementation	
IP1	5′-ATAAGAATGCGGCCGCTCCGCTTCCTTTAGCAGCC-3′; forward primer for inverse PCR of pFNLTP7	
IP2	5′-ATAAGAATGCGGCCGCTTAAGCATTGGTAACTGTCAGA-3′; reverse primer for inverse PCR of pFNLTP7	
K1	5′-GCTATTCGGCTATGACTG-3′; forward primer for 634-bp kanamycin marker (*aphA2*) probe	
K2	5′-CAGCAATATCACGGGTAG-3′; reverse primer for 634-bp kanamycin marker (*aphA2*) probe	
K3	5′-GCTTCCTCGTGCTTTACGG-3′; *aphA-2* primer for *HimarFT* insertion sequencing	
R1	5′-TGCCACCTAAATTGTAAGCG-3′; R6K primer for *HimarFT* insertion sequencing	
T1	5′-CGTCGATATGTAACAATGG-3′; forward primer for 578-bp transposase (*tnp*) probe	
T2	5′-CCTTCAAGAGCGATACCAC-3′; reverse primer for 578-bp transposase (*tnp*) probe	
WA1	5′-CCGCTCGAGAATCCATGCTATGACTGATGC-3′; forward primer for 2.4-kb *wbtA* fragment for complementation	
WA2	5′-CCGCTCGAGGCTTATCTTTACCATATCGC-3′; reverse primer for 2.4-kb *wbtA* fragment for complementation	
WM1	5′-CCGCTCGAGATCTGCGCAGTAATGACAGG-3′; forward primer for 1.7-kb *wbtM* fragment for complementation	
WM2	5′-CCGCTCGAGAAATCTTGGCTATATGATGGCA-3′; reverse primer for 1.7-kb *wbtM* fragment for complementation	

[a] Km^r, Ap^r, and Nt^r indicate resistance to kanamycin, ampicillin, and nourseothricin, respectively.
[b] The underlined regions are restriction enzyme sites for BamHI (primer H3), NotI (primers IP1 and IP2), and XhoI (primers H4, WA1, WA2, WM1, and WM2).

In this paper, we report the results of *Himar1*-based transposon (*HimarFT*) mutagenesis of *F. tularensis* LVS obtained utilizing a screen for isolates defective for cytopathogenicity in cultured J774A.1 macrophages. Genes with predicted functions that include a variety of transport processes, metabolic functions, capsule and LPS biosynthesis, posttranslational modification, and protein turnover, as well as hypothetical genes with unknown functions, were identified. Insertions in seven hypothetical genes resulted in strains that were attenuated for growth to various extents in macrophages and within mice in vivo. None of these mutants were defective for macrophage entry. One open reading frame for a predicted hypothetical membrane protein was identified as a gene involved in LPS biosynthesis in *F. tularensis* LVS and Schu S4.

MATERIALS AND METHODS

Bacterial strains, plasmids, and growth conditions. All bacterial strains and plasmids used in this study are listed in Table 1. Studies involving type A *F. tularensis* strain Schu S4 were carried out under biosafety level 3 conditions according to federal and institutional select agent regulations. *F. tularensis* subspecies were routinely grown at 37°C in 2.1% Mueller-Hinton (MH) medium supplemented with glucose, iron, and IsoVitaleX as described previously (41). MH broth contained 1.24 mM $CaCl_2$ and 1.03 mM $MgCl_2$, and MH agar contained 0.5% NaCl, 1.6% agar, 1% tryptone (MHT) or protease peptone (MHP), and 2.5% calf or fetal bovine serum (Invitrogen, Carlsbad, CA). For in vivo infections, inocula were prepared in MHP broth. In some experiments, Chamberlain's chemically defined medium (CDM) was used (10). When required, medium was supplemented with kanamycin (10 μg ml^{-1}) or nourseothricin (5 μg ml^{-1}). Selection for nourseothricin resistance was performed at 30°C. *Escherichia coli* was grown aerobically at 37°C in Luria-Bertani medium supplemented with kanamycin (50 μg ml^{-1}) or nourseothricin (50 μg ml^{-1}) when required. Kanamycin was purchased from United States Biochemical Corporation (Cleveland, OH), and nourseothricin was purchased from WERNER BioAgents (Jena, Germany).

DNA manipulation and transformation. Purification and manipulation of plasmid or genomic DNA, electroporation of *F. tularensis*, and chemical transformation of *E. coli* were performed as described previously (41). Custom oligonucleotide primers (Table 1) were synthesized by Operon (Huntsville, AL). DNA maps were constructed using MacPlasmap Pro 3.01 (CGC Scientific, Inc., Ballwin, MO). To determine insertion locations in *F. tularensis* LVS, genomic DNA from each strain was digested with SpeI and treated with T4 DNA ligase. *HimarFT*-containing fragments were recovered as plasmid DNA in *E. coli* DH5α*λpir* and subsequently used as a template for sequencing (9). Insertion locations for *F. tularensis* Schu S4 single- and double-crossover strains with mutations in FTT1238c were determined by sequencing directly from genomic DNA. Sequencing reactions and analysis were performed as described previously (41). Southern blotting of SpeI-digested genomic DNA was performed as described previously using either the Random Prime DNA labeling system (Invitrogen) and [α-^{32}P]dCTP or a digoxigenin High Prime DNA labeling and detection starter kit (Roche Diagnostics Corporation, Indianapolis, IN). Probes constructed for identification of the aminoglycoside 3′-phosphotransferase (*aphA-2*) (64), the transposase (*tnp*), or the N terminus of FTL_0706 are described in Table 1.

Genome and bioinformatic analyses. The *HimarFT* insertion site sequences were compared with the *F. tularensis* LVS genome (accession no. NC_007880) at http://bbrp.llnl.gov/bbrp/bin/f.tularensis_blast and the *F. tularensis* Schu S4 genome (NC_006570) available at http://www.ncbi.nlm.nih.gov/entrez/query.fcgi?db=genome&cmd=Retrieve&dopt=Overview&list_uids=563. Additional *F. tularensis* subsp. genomic comparisons were performed using www.francisella.org.

Further analysis and annotation of candidate proteins were performed using the high-resolution tools PhyloBlocks (http://compbio.mcs.anl.gov/ulrich/phyloblock/) and Dragonfly (http://compbio.mcs.anl.gov/dragonfly/) available via the PUMA2

system (43). Candidate sequences were analyzed using BLAST, InterPro, SignalP, and TMHMM to identify global sequence alignments, local conserved domains, potential signal sequences, and potential transmembrane domains, respectively (1, 5, 47, 48). The results of these analyses were used to assign potential functions to the genes. Further identification of the conserved regions specific for predicted functions was done using PhyloBlocks. In brief, a set of orthologous sequences identified by BLAST were aligned using ClustalW and analyzed by Block Maker for prediction of the conserved motifs (31). Consensus sequences and HMM profiles were also generated for these sets of orthologs to be used for future analysis and classification.

Western blot analysis. Whole-cell lysates (1×10^9 cells in 100 μl) were boiled for 5 min in loading buffer, and 5 μl of each sample was loaded and separated on 10% polyacrylamide-sodium dodecyl sulfate gels. Western transfer, blocking, and antibody incubation were performed as described previously (41). Treatment with the mouse monoclonal anti-*F. tularensis* LPS primary antibody (1:8,000 dilution; Advanced ImmunoChemical Inc.) was followed by treatment with a horseradish peroxidase-conjugated goat anti-mouse immunoglobulin G secondary antibody (1:10,000 dilution; Roche).

***F. tularensis* LVS *HimarFT* library construction.** The pHimar H3 construct is a modified *HimarFT* suicide delivery vehicle constructed from temperature-sensitive pFNLTP16 H3 (42). Transposition using pHimar H3 was performed by electroporation of 100 ng of DNA into electrocompetent *F. tularensis* LVS. After outgrowth at 37°C on a shaker for 4 h, dilutions were plated onto MHT agar containing kanamycin and incubated at 37°C to select for *HimarFT*. In addition, dilutions were plated onto MHT agar without kanamycin to determine the total number of potential recipients. Colonies grown for 3 or 4 days at 37°C were picked, struck onto MHT agar containing kanamycin, and grown at 37°C to recover individual clones containing *HimarFT* insertions in the genome. For *HimarFT* library construction and storage, Km^r colonies were placed into 0.5 ml MH broth containing kanamycin in tissue culture plates with 96 deep wells. The last row in each plate was not inoculated as a control. Sterile lids and Parafilm were used to cover the plates for incubation and freezer storage. After 2 days of growth at 37°C and 200 rpm, 0.5 ml sterile 30% glycerol was added and mixed into each well to obtain a final glycerol concentration of 15%, and the plates were stored at −80°C. Recovery of the library was performed by using a 96-pin replicator and square agar plates (Nalge Nunc International Corp., Rochester, NY) containing MHT agar with kanamycin.

***HimarFT* library screen utilizing a macrophage infection model.** Stage 1 screening with J774A.1 macrophages (ATCC TIB-67) was performed using a 96-well format with a multiplicity of infection (MOI) of ~50 to 200. Macrophages were seeded at a concentration of 6×10^4 cells per well and incubated overnight at 37°C in 5% CO_2 before infection. Strains containing transposon insertions were grown on MHT agar with kanamycin for 3 days at 37°C and for 0 to 2 days at room temperature and transferred into a 96-well plate containing 100 μl of Dulbecco's modified Eagle's medium (DMEM) (Sigma-Aldrich, St. Louis, MO) supplemented with 10% fetal bovine serum and 4 mM L-glutamate (Invitrogen). The DMEM was aspirated from the macrophages, and 50-μl portions of test bacterial suspensions were placed onto macrophages. These steps were performed one row at a time to minimize drying of the monolayers. A 2-h incubation at 37°C in the presence of 5% CO_2 was performed to allow bacterial attachment and entry. Each row of eight wells was then aspirated to remove the extracellular organisms, washed with 200 μl of Hanks' balanced salt solution, and aspirated again, and the contents were replaced with 200 μl of DMEM containing 5 μg ml^{-1} of gentamicin (Invitrogen) to kill extracellular bacteria. The plates were then incubated at 37°C in the presence of 5% CO_2 for 2 days. Candidates, which retained the macrophage monolayer similar to uninoculated controls (groups A and B), were subjected to a second-stage 24-well analysis with 3.7×10^5 macrophages per well and defined inocula normalized using optical density to obtain an MOI of 100.

Crystal violet staining of J774A.1 macrophages. The integrity of the macrophage monolayer was assessed by crystal violet staining. DMEM was aspirated from the macrophages, and the monolayers were washed with phosphate-buffered saline and then incubated with a 1% crystal violet solution for 5 min at room temperature. The crystal violet was removed, and the macrophage monolayers were washed with distilled water and allowed to dry before visual assessment of the stain intensity. Crystal violet was purchased from Hardy Diagnostics (Santa Maria, CA).

Quantitation of *Francisella* cytotoxicity with J774A.1 macrophages by LDH release. The release of cytosolic lactate dehydrogenase (LDH) into the supernatant of infected cells was used as an indicator for lysis (CytoTox96; Promega Corporation, Madison, WI). Bacterial cell suspensions were prepared and normalized to an MOI of 100 based on the optical density at 550 nm (OD_{550}) and subsequent plating to determine the actual number of CFU ml^{-1}. The conditions used for J774A.1 macrophage infection were the same as those used for the 24-well stage 2 cytopathic screening. At 48 h postinfection, supernatants were harvested and the maximum lysis was determined (by addition of 100 μl of lysis buffer to an uninfected monolayer with 900 μl DMEM and incubation at 37°C for 45 min). Uninfected medium was used as a background control, and suitable dilutions of the other samples were included. The release of LDH was determined by measuring the OD_{490} using a plate reader and softmax pro software (Molecular Devices Corporation, Sunnyvale, CA).

Growth analysis of *F. tularensis* LVS mutants in bacteriological medium. Growth in MH or CDM broth was assessed using a 96-well format with a plate reader and softmax pro software. One test colony was emulsified in 100 μl of CDM broth, 10 μl was placed into 190 μl of MH or CDM broth, and the microtiter plate was incubated at 37°C with shaking at 100 to 200 rpm. Turbidity changes in the cultures were monitored at OD_{550} for 24 h (data not shown). Some strains were grown on MH or CDM agar to confirm the observed phenotypes in broth.

In vivo analysis of *HimarFT* insertion mutants. Six- to 8-week-old female BALB/c mice (Harlan Sprague Dawley, Inc., Indianapolis, IN) were infected by intraperitoneal (i.p.) injection of 0.1 ml (final volume) of phosphate-buffered saline containing the *F. tularensis* LVS wild type or mutant derivatives. The inocula were prepared from MHP broth cultures in the exponential phase of growth, and the concentrations were adjusted so that they represented approximately 1,000 50% lethal doses (21, 29). The actual number of bacteria delivered was determined by performing plate counts of the inoculum on MHP agar. Infected animals were closely monitored for 21 days, and the number of moribund animals during this time was determined. Animal infection experiments were approved by the Institutional Animal Care and Use Committee and the Institutional Biosafety Committee of the Medical College of Wisconsin.

Complementation of selected *HimarFT* mutant strains using pFTNAT. The complementation plasmid pFTNAT was constructed by inverse PCR using primers IP1 and IP2 (Table 1) and pFNLTP7 as the template DNA (41). Both the kanamycin and ampicillin resistance genes were removed, and the nourseothricin resistance marker was inserted at a NotI site (26). The pFTNAT plasmid retains the ability to replicate in both *E. coli* and *F. tularensis*. The complementation plasmids pFTNAT-FTL_0706, pFTNAT-$wbtA_{LVS}$, and pFTNAT-$wbtM_{LVS}$ were constructed by PCR amplification of genomic DNA with primer pairs H3/H4, WA1/WA2, and WM1/WM2 (Table 1), respectively, resulting in gene fragments with 175-, 472-, and 481-bp upstream sequences (putative promoter regions). All fragments were ligated into pCR-Blunt II-TOPO and subsequently subcloned into pFTNAT using EcoRI, XhoI, and XhoI, respectively.

RNA isolation and RT-PCR analysis of *F. tularensis HimarFT* strains with insertions in *wbtA*. RNA was isolated using an RNeasy Protect mini kit (QIAGEN). Isolated RNA was treated with DNase I (Fermentas Inc., Hanover, MD) to remove contaminating genomic DNA for 1 h at 37°C and subsequently purified with the RNeasy Protect mini kit. RNA quality was verified by agarose gel analysis. Reverse transcription (RT)-PCR was performed using the SuperScript III One-Step RT-PCR system with Platinum *Taq* DNA polymerase (Invitrogen). Control PCRs were performed with Platinum *Taq* High Fidelity DNA polymerase (Invitrogen). Primers C1, C2, D1, and D2 were used for mRNA detection of either a 366-bp fragment of *wbtC* or a 410-bp fragment of *wbtD* downstream of *wbtA* (Table 1). All reaction mixtures included 50 ng of template DNA or RNA and were incubated at 50°C for 30 min for RT, followed by PCR for 25 cycles.

Statistical analysis. Statistical significance was determined using single-factor analysis of variance.

RESULTS

Transposon mutagenesis of *F. tularensis* LVS using *HimarFT*. In previous studies, a temperature-sensitive plasmid and a modified *Himar1* transposon (*HimarFT*) were developed to perform random mutagenesis in *F. tularensis* (41, 42). While this system resulted in random, single, stable insertions without orientation bias, a drawback was observed when large-scale experiments were performed to saturate the genome. We noted that plasmid sequences were retained at a variable frequency. The failure to lose plasmid sequences may have been due to the length of time required for the plates to achieve the restrictive temperature, the number of generations required to dilute nonreplicating DNA, or the reversion of the point mutation in the replication initiation protein encoded by *repA*.

Sequencing of *repA* from five isolates retaining the plasmid sequence confirmed the maintenance of the temperature-sensitive mutation. Plasmid rearrangements were not observed (data not shown). We noted that plasmid sequences were lost if strains were passaged at the restrictive temperature two additional times (49).

To avoid the labor-intensive steps of passaging individual isolates, the delivery vehicle was modified by removing the NotI fragment encoding pFNLTP16 to construct pHimar H3 (Fig. 1A). Deletion of the replicon for *Francisella* converted pFNLTP16 H3 to a suicide delivery system for *HimarFT*. The efficiency of transposition with pHimar H3 was similar to that obtained for pFNLTP16 H3, with $\sim 2 \times 10^{-5}$ insertion per cell. The stable retention of *HimarFT* and the loss of plasmid sequences were confirmed by examining 100 mutagenized strains by colony blot analysis with ^{32}P-labeled probes hybridizing to the aminoglycoside 3′-phosphotransferase (*aphA-2*) responsible for kanamycin resistance and the transposase (*tnp*), respectively. Southern blot analysis with genomic DNA isolated from 10 mutants after transposition demonstrated that there were random, single insertions and loss of the plasmid vehicle (Fig. 1B and data not shown). For construction of the insertion library, *F. tularensis* LVS was mutagenized with pHimar H3 and approximately 7,000 kanamycin-resistant colonies were arrayed into microtiter plates with 96 deep wells and preserved at −80°C.

Isolation of mutants with insertions in *Francisella* genes required for virulence in J774.A1 macrophages. *Francisella* enters, replicates, and causes apoptosis-induced cytopathogenicity within macrophages (44, 51, 65). To screen for genes required for *F. tularensis* LVS virulence in J774.A1 macrophages, the integrity of macrophage monolayers infected with individual Km^r clones was assessed by staining with crystal violet. Preliminary experiments indicated that crystal violet staining at 2 days after infection at an MOI of 100 was optimal for the detection of cytopathogenicity (Fig. 2A). The initial screening (stage 1) was performed with an estimated MOI of 50 to 200 using a 96-well format. The retention of the monolayer and dark staining suggested that the clones were unable to enter, replicate, or cause apoptosis during the 2-day incubation. Noncytopathic candidates were retested in duplicate (stage 2) in 24-well plates at an MOI of 100 (Fig. 2B). Mutants were categorized into four groups based on staining intensity: no loss of the monolayer, as in the uninfected control well (group A), a small but detectable loss of monolayer (group B), detectable loss of cells (group C), and severe monolayer destruction, similar to that obtained with the parental strain, *F. tularensis* LVS (group D). To cull putative auxotrophs or other mutants defective in general metabolism, 140 candidates appearing to possess the most attenuated phenotypes (groups A and B) in macrophages were characterized for growth in complex and minimal bacteriological media (stage 3 screening) (data not shown). Duplicate cultures for each strain were arrayed in 96-well plates in MH or CDM broth, and growth was monitored over time by assessing the increase in optical density. Colony morphology was assessed using cultures transferred from microtiter broth cultures to MHT or CDM agar plates. Twenty-four strains failed to grow in or on CDM and are likely auxotrophic strains. Slower growth or inconsistent growth patterns were observed for another 24 candidates. In

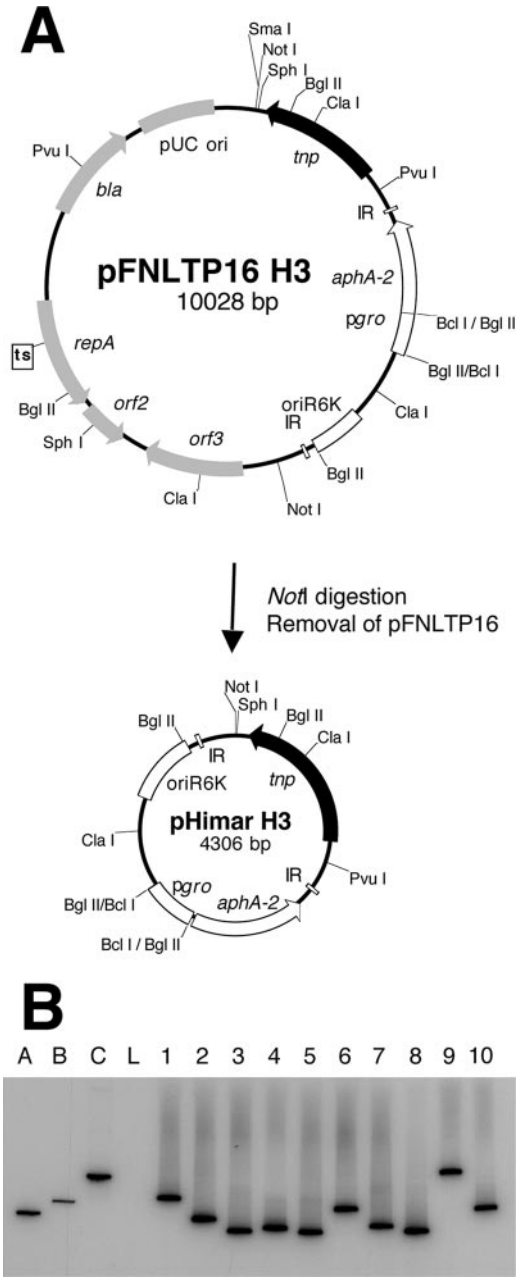

FIG. 1. (A) Construction of a suicide delivery vehicle for *HimarFT* transposition. The original *HimarFT* transposon with the *Francisella groEL* promoter (p*gro*) facilitating expression of the aminoglycoside 3′-phosphotransferase (*aphA-2*) and transposase (*tnp*) genes on the temperature-sensitive pFNLTP16 vehicle is shown. pHimar H3 was constructed by removal of the NotI fragment containing pFNLTP16. (B) Verification of pHimar H3 insertion in *F. tularensis* LVS by Southern blot analysis of SpeI-digested genomic DNA. Hybridization with a ^{32}P-labeled probe specific to *aphA-2* was observed for 10 representative strains after pHimar H3 mutagenesis. Wild-type *F. tularensis* LVS genomic DNA (lane L) was included as a negative control. Three plasmids were included as markers (42): pMiniHimar (4 kb) (lane A), pFNLTP1 (6.9 kb) (lane B), and pFNLTP16 H3 (10 kb) (lane C). A probe specific to the transposase (*tnp*) gene on the plasmid did not hybridize with genomic DNA but produced a signal for markers A and C (data not shown).

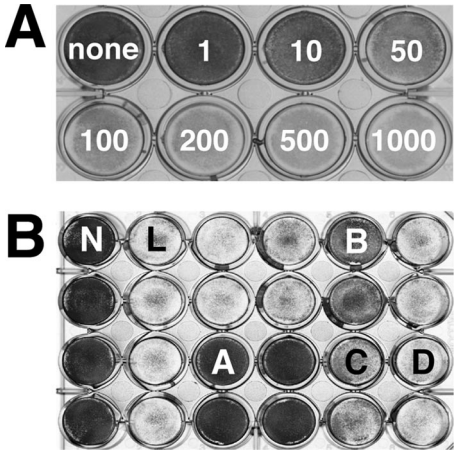

FIG. 2. (A) Crystal violet staining of J774A.1 macrophages infected with *F. tularensis* LVS at various MOIs 2 days postinfection. The retention of the J774A.1 macrophage monolayer after infection is compared to the uninfected control (none). (B) *F. tularensis* LVS *HimarFT* mutant stage 2 macrophage screening using an MOI of 100. The uninfected control (well N) retains the monolayer and stains dark, while wild-type *F. tularensis* LVS (well L) is cytopathic, causing loss of the monolayer. Based on crystal violet retention, strains with *HimarFT* insertions were classified into four groups (A to D) represented by wells A to D, respectively: group A, similar to uninfected controls; group B, intermediate dye retention; group C, light dye retention; and group D, no dye retention, similar to infection by the parental strain. Phenotypes corresponding to groups A and B were characterized further.

summary, the combined screens identified 89 strains with *HimarFT* insertions in genes potentially important for virulence in macrophages.

Identification of the site of *HimarFT* insertion. To recover DNA flanking the *HimarFT* insertion site, genomic DNA from each of the 89 candidates was digested with SpeI, ligated, and transformed into *E. coli* DH5α*λpir*. Of the 89 genomes, 70 (79%) were recovered as independently replicating plasmids containing *HimarFT* and adjacent genomic DNA, an efficiency similar to that reported elsewhere for transposons in *Francisella* (69). Recovered plasmids were used as templates for nucleic acid sequencing reactions with primers specific for *HimarFT* sequences corresponding to *aphA-2* and the R6K origin (Table 1 and Fig. 1A). From this analysis, 26 unique genes were identified. Known or predicted functions for these genes included transport processes, metabolism of nucleotides, carbohydrates, amino acids, and coenzymes, capsule and LPS biosynthesis, and posttranslational modification/protein turnover (Table 2). The recovery of several *HimarFT* insertions in genes previously found to have a role in macrophage growth, including the caseinolytic protease gene *clpB*, the disulfide bond-related gene *dsbB*, the aspartate aminotransferase gene *aspC2*, and the putative capsular genes *capBC* and *wbtA* involved in O-antigen biosynthesis, validated the screening process used (28, 55, 58, 63, 67, 69, 70, 76). Several hypothetical

TABLE 2. *F. tularensis* LVS *HimarFT* mutant strains attenuated for growth in macrophages[a]

Gene[b]	Gene locus		No. of insertions/gene[c]	Protein product
	LVS	Schu S4		
	FTL_1806	FTT0053	2	Major facilitator superfamily transporter
dsbB	FTL_1670	FTT0107c	1	Disulfide bond formation protein, DsbB
glgB	FTL_0483	FTT0413c	5	Glycogen branching enzyme, GlgB; polysaccharide metabolism
xasA	FTL_1583	FTT0480c	4	Glutamate-aminobutyric acid antiporter, XasA; amino acid transport
	FTL_0878	FTT0610	1	DNA/RNA endonuclease family
	FTL_0886	FTT0618c	1	Conserved hypothetical protein YleA; possible tRNA-i (6)A37 methylthiotransferase
capB	FTL_1416	FTT0805	3	Capsule biosynthesis protein CapB
capC	FTL_1415	FTT0806	1	Capsule biosynthesis protein CapC
	FTL_1414	FTT0807	2	Hypothetical protein; possible capsule-related protein
	FTL_0439	FTT0919	2	Hypothetical outer membrane protein
	FTL_1262	FTT0945	1	Chorismate family binding protein; aromatic amino acid and folate biosynthesis
	FTL_1096	FTT1103	1	Hypothetical lipoprotein; ABC transporter and potential disulfide bond formation protein, DsbA
metN	FTL_0838	FTT1124	5	D-Methionine transport protein (ABC transporter), MetN
metIQ	FTL_0837	FTT1125	9	D-Methionine transport protein (ABC transporter), MetIQ
aspC2	FTL_0789	FTT1165c	3	Aspartate aminotransferase; amino acid biosynthesis
ggt	FTL_0766	FTT1181c	7	Gamma-glutamyltranspeptidase; amino acid, arachidonic acid, and glutathione metabolism
	FTL_0706	FTT1238c	3	Hypothetical membrane protein; LPS biosynthesis
wbtM	FTL_0606	FTT1450	1	dTDP-glucose 4,6-dehydratase, WbtM, O-antigen polysaccharide biosynthesis
wbtC	FTL_0594	FTT1462c	1	UDP-glucose-4-epimerase, WbtC, O-antigen polysaccharide biosynthesis
wbtA	FTL_0592	FTT1464c	5	dTDP-glucose 4,6-dehydratase, WbtA, O-antigen polysaccharide biosynthesis
	FTL_0304	FTT1490	4	Na^+/H^+ antiporter; regulation of pH
	FTL_0544	FTT1564	1	Hypothetical protein; polyphosphate kinase
gplX	FTL_1701	FTT1631c	1	Fructose-1,6-bisphosphatase, GplX, glucose metabolism
	FTL_0050	FTT1645	1	Hypothetical protein; major facilitator superfamily
	FTL_0058	FTT1688	3	Aromatic amino acid transporter of HAAAP family
clpB	FTL_0094	FTT1769c	2	Caseinolytic protease, ClpB; response to unfolded protein

[a] Gene designations, loci, and protein designations correspond primarily to those in the Schu S4 genome annotation (http://www.ncbi.nlm.nih.gov/entrez/query.fcgi?db=genome&cmd=Retrieve&dopt=Overview&list_uids=563). This gene list was compared with the *F. tularensis* LVS genome at www.francisella.org. Additional bioinformatics was performed by the Computational Biology Group at Argonne National Laboratory (indicated after the semicolon for some candidates). Hypothetical candidates are underlined.

[b] The gene corresponds to the annotated gene designation if available.

[c] The number of insertions per gene corresponds to the number of sequenced *HimarFT* insertions per open reading frame.

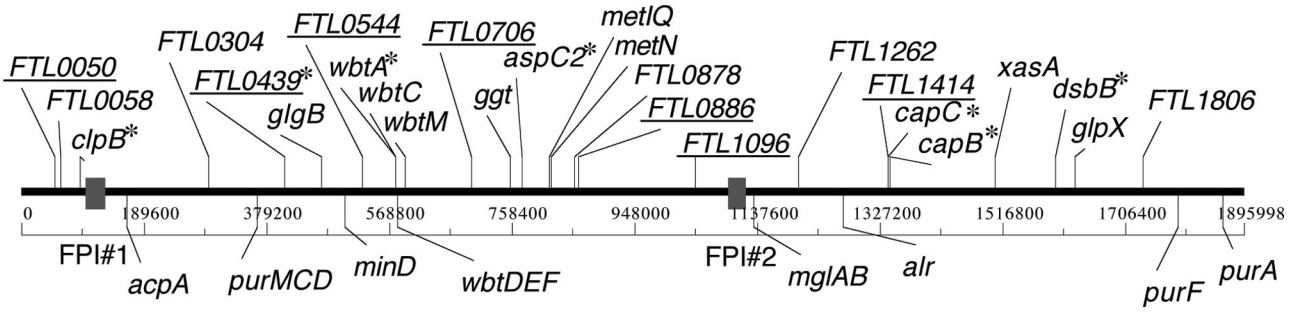

FIG. 3. *F. tularensis* LVS genomic map of *HimarFT* insertion mutants recovered after stage 2 and 3 screening (designations above the *F. tularensis* LVS genome). Hypothetical *HimarFT* mutants are underlined. Several genes previously reported to be involved in growth inside macrophages were recovered, including *clpB*, FTL_0439, *wbtA*, *capBC*, *aspC2*, and *dsbB* (designated by asterisks; above the *F. tularensis* LVS genome). Regions and genes previously shown to be involved in macrophage growth but not recovered as strongly attenuated after the screening of our *HimarFT* library are indicated by the gray boxes corresponding to the *Francisella* pathogenicity islands (FPI#1 and FPI #2) and below the *F. tularensis* LVS genome, respectively.

proteins were also identified. Insertions appeared to be spread evenly throughout the genome (Fig. 3).

In vivo analysis of mutants containing transposon insertions in genes encoding hypothetical proteins. To focus on new gene discovery, strains with insertions in hypothetical genes were selected to test for attenuation in vivo. Groups of five BALB/c mice were given an intraperitoneal (i.p.) injection of mutant derivatives at doses ranging from 1,000 to 5,000 CFU or 3 logs above the reported 50% lethal dose (21, 29). Previous work indicated that BALB/c mice are moribund by day 4 to 8 when they are infected i.p. with 50 CFU or less (39, 53). Mice infected with strains bearing insertions in the hypothetical genes tested survived throughout the 21 days of monitoring (Table 3). We also challenged mice with *F. tularensis* FTL_0741::*HimarFT*, with a transposon insertion in a hypothetical locus that exhibited a parental phenotype in vitro. In vivo, LVS FTL_0741::*HimarFT* exhibited a parental phenotype, while LVS Δ*purMCD* failed to induce active infection (53). These results suggest that a *HimarFT* insertion generates a specific phenotype related to its location in the chromosome.

Characterization of transposon mutants for entry, initial replication, and cytotoxicity. Attenuation in vivo for all mutants tested suggested that the in vitro cellular assay results correlated with pathogenicity. To determine if quantitative defects were associated with different stages of infection, mutants with insertions in hypothetical genes were tested with J774A.1 macrophages to determine their capacities to enter, replicate, and cause the release of LDH, an indicator of cell death (Fig. 4). An intracellular replication-deficient mutant used as a control, *F. tularensis* LVS Δ*purMCD*, exhibited reduced replication and cytotoxicity, consistent with its attenuation in mice (53). Similarly, inactivation of FTL_0741 resulted in no change in replication and cytotoxicity, consistent with the wild-type phenotype in mice. There was no significant difference between LVS and the strains bearing *HimarFT* insertions in terms of the ability to enter J774A.1 macrophages (Fig. 4A). Statistically significant differences ($P < 0.05$) from the parental strain were observed when replication at 24 h and cytotoxicity at 48 h for mutants with insertions in FTL_0886, FTL_1414, FTL_0439, FTL_0706, and FTL_0050 were examined (Fig. 4B and C), consistent with the attenuation of these mutants in mice. Thus, defects in macrophage replication generally correlate with the inability to induce cytotoxicity. Interestingly, LVS FTL_0544::*HimarFT* displayed no significant changes in either cytotoxicity or replication, despite being attenuated in mice, compared to the wild type (Fig. 4B and C).

TABLE 3. BALB/c mice challenged with *F. tularensis* LVS hypothetical *HimarFT* mutants

Strain	Mutant challenge (CFU)[a]	No. of mice surviving mutant challenge/ total no. of mice[b]
LVS	5,200	0/5
LVS Δ*purMCD*	2,200	5/5
LVS FTL_0886	1,010	5/5
LVS FTL_1414	2,180	5/5
LVS FTL_0439	5,100	5/5
LVS FTL_1096	2,850	5/5
LVS FTL_0741	1,990	0/5
LVS FTL_0706	1,560	5/5
LVS FTL_0544	2,640	5/5
LVS FTL_0050	3,900	5/5

[a] Mice were inoculated i.p. (0.1 ml) with 1,000 to 5,000 CFU of *F. tularensis* LVS *HimarFT* hypothetical (FTL) mutants. The mutant challenge was determined by counting CFU on MHP agar.

[b] Survival was determined 21 days after infection. Mice challenged with *F. tularensis* LVS and LVS FTL_0741::*HimarFT* died 3 to 8 days after infection.

LPS phenotype of selected *HimarFT* mutant strains. LPS biosynthesis has been previously shown to be important for intracellular replication (13, 58, 63, 70). Loss of a functional copy of *wbtA* results in loss of the O-antigen ladder (58, 63). Five *F. tularensis* LVS *wbtA*::*HimarFT* mutants from this study exhibited loss of O antigen, as predicted (Fig. 5A). Two additional mutations in the *wbt* locus, with *HimarFT* insertion in either *wbtM* or *wbtC*, resulted in complete O-antigen loss and loss of low-molecular-weight O antigen, respectively (Fig. 5A). These phenotypes have not been previously reported and likely correlate to the location in the pathway of LPS biosynthesis. Other mutations in the *wbt* locus, such as *wbtDEF* mutations, also result in a lack of O antigen (70). Strains with insertions in predicted capsule-related genes retained the O-antigen ladder, suggesting that mutation of these genes does not affect LPS (Fig. 5B). *HimarFT* mutations within hypothetical genes were analyzed by Western blotting to assess whether any of these

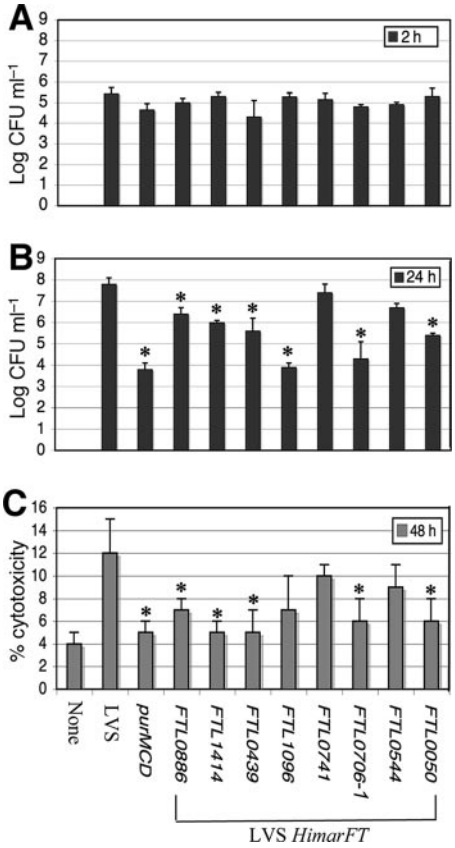

FIG. 4. (A and B) Entry and replication in J774A.1 macrophages of the *F. tularensis* LVS wild type and Δ*purMCD*, FTL_0741::*HimarFT*, and attenuated mutants with insertions in loci encoding hypothetical proteins. The experiments were performed using a 24-well format with an MOI of 100 in triplicate. The results are expressed as mean log CFU ml^{-1}; the error bars indicate standard deviations. Mutants found to be significantly impaired in entry at 2 h or in replication at 24 h are indicated by asterisks ($P < 0.05$). (C) Quantitation of cytotoxicity by measuring LDH release into the supernatant compared to an uninfected monolayer (maximum lysis) at 48 h. LDH release was monitored alongside assessment for entry and replication defects as described above for panels A and B. Experiments were performed in triplicate, The bars indicate mean percentages of cytotoxicity, and the error bars indicate standard deviations. Mutants found to have a significant reduction in the percentage of cytotoxicity at 48 h are indicated by asterisks ($P < 0.05$).

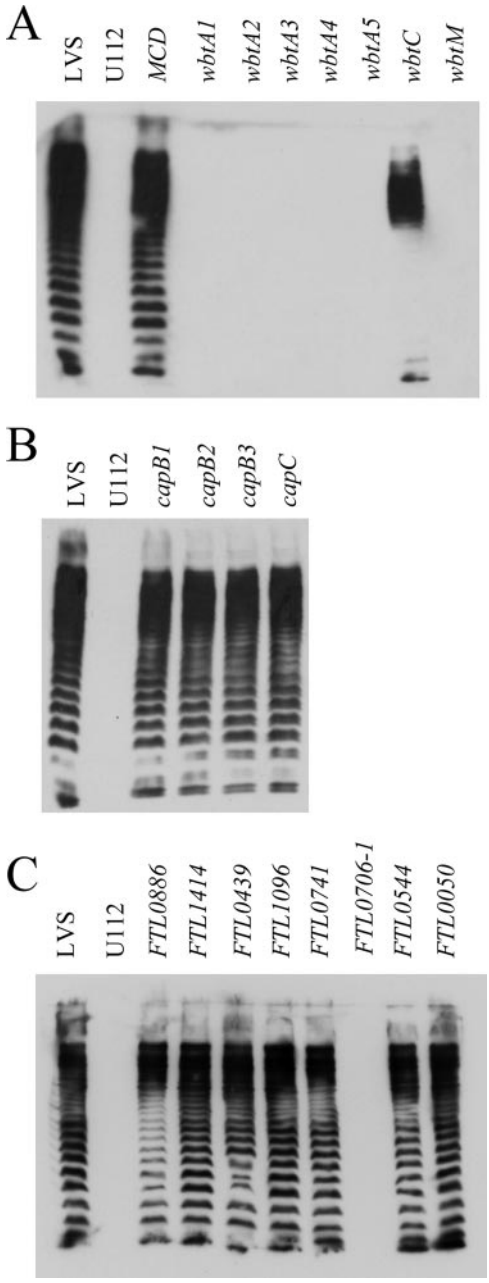

FIG. 5. Western blot analysis of *F. tularensis* LVS or *F. novicida* U112 cell lysates with a mouse monoclonal anti-*F. tularensis* LPS antibody. The antibody recognizes LPS from *F. tularensis* LVS and Schu S4 but not LPS from *F. novicida* U112. Each *HimarFT* mutant strain is indicated by the gene in which *HimarFT* insertion was mapped, as shown in Table 2. Multiple strains with mutations in the same gene are indicated by the gene designation and a candidate number. The previously studied *F. tularensis* LVS Δ*purMCD* mutant is indicated by *MCD* (53).

genes represent unrecognized LPS biosynthetic genes. All of the insertions in hypothetical genes resulted in a parental pattern for the O-antigen side chain except for LVS FTL_0706::*HimarFT* (Fig. 5C). We concluded that the hypothetical protein encoded by FTL_0706 likely functions in the LPS biosynthetic pathway.

Complementation and *HimarFT* polarity. *HimarFT* was engineered to contain a strong constitutive *groEL* promoter to transcribe the *aphA-2* kanamycin resistance marker. Transcriptional stop sequences were not added, raising the possibility that the orientation of insertion may affect the transcription of adjacent genes. *HimarFT* mutants with insertions mapped to the beginning (*wbtA*) and the end (*wbtM*) of the *wbt* region were used to determine if the orientation of *HimarFT* influenced either the complementation pattern or transcription of downstream genes (Fig. 6A). Gene expression analyses were performed with *F. tularensis* LVS *wbtA1*::*HimarFT* and *wbtA2*::*HimarFT*, in which *HimarFT* had been mapped in the two orientations (Fig. 6A). To detect the presence of mRNA downstream of *wbtA*, RT-PCR was performed with primers designed to detect message containing *wbtC* or *wbtD* (Fig. 6A).

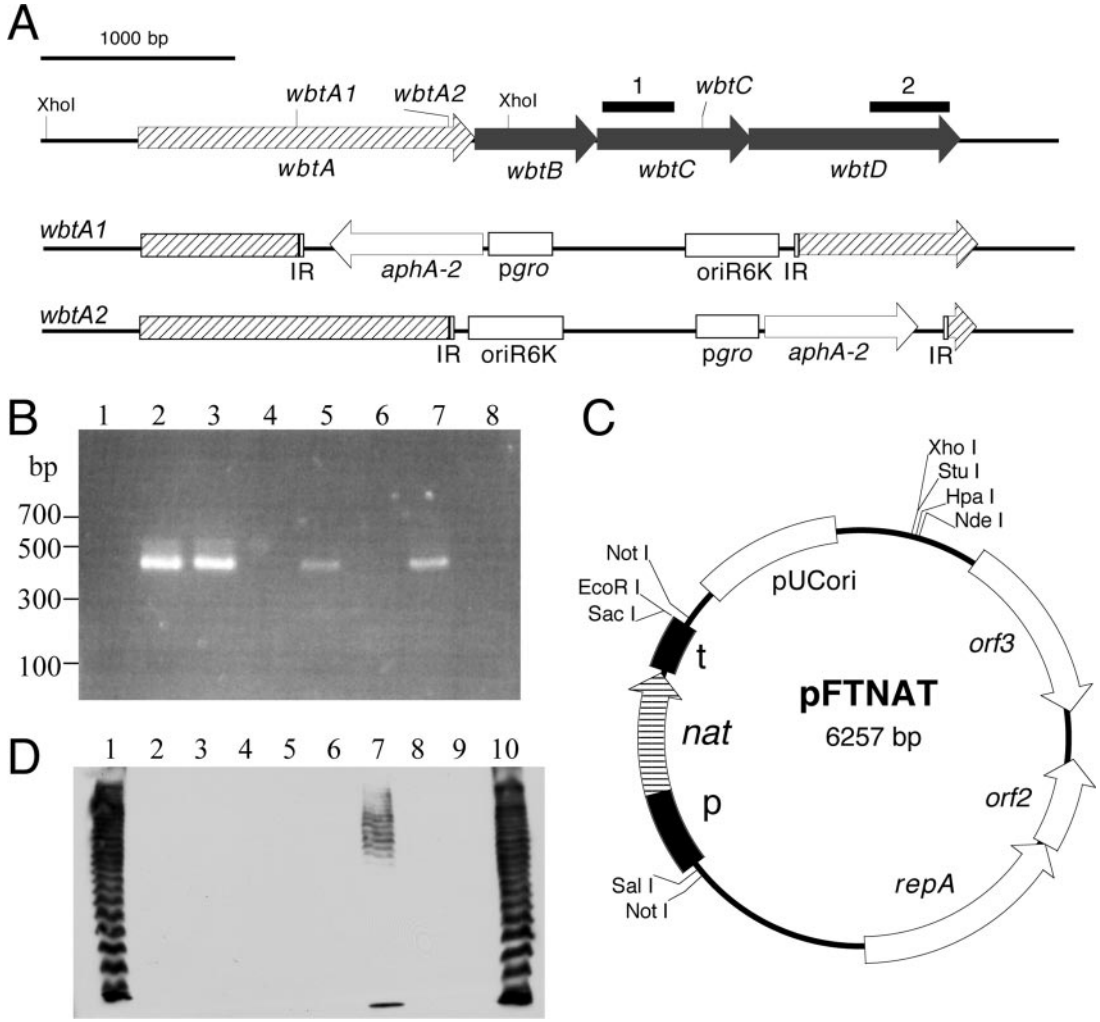

FIG. 6. Analysis of *F. tularensis* LVS *HimarFT* strains with mutations in the *wbt* locus by RT-PCR and complementation. (A) Map of the *wbt* loci (FTL_0592 to FTL_0595) in the *F. tularensis* LVS genome. The *HimarFT* insertion sites are indicated for *F. tularensis* LVS *wbtA1*::*HimarFT*, *wbtA2*, and *wbtC* mutant strains (indicated by the gene designation and candidate number). FTL_0606 (*wbtM*) is just downstream of the main *wbt* operon (FTL_0592 to FTL_0605). The genomic region used for complementation of the *wbtA* mutants is between the XhoI sites. Bars 1 and 2 correspond to the regions selected for detection of mRNA downstream of *wbtA* by RT-PCR. *HimarFT* insertion site maps for *F. tularensis* LVS *wbtA1*::*HimarFT* and *wbtA2*::*HimarFT* are shown, with LVS *wbtA2*::*HimarFT* containing the *groEL* promoter (p*gro*) in the same orientation as the gene. (B) Detection of mRNA containing *wbtD* downstream of *wbtA* in LVS *wbtA1*::*HimarFT* and *wbtA2*::*HimarFT* by RT-PCR. The reaction and template conditions used included RT-PCR with no template (lane 1), LVS genomic DNA (lane 2), and RNA isolated from either LVS wild-type (lane 3), *wbtA1*::*HimarFT* (lane 5), or *wbtA2*::*HimarFT* (lane 7). Control RT-PCRs without the reverse transcriptase were performed using RNA from LVS wild-type (lane 4), *wbtA1*::*HimarFT* (lane 6), and *wbtA2*::*HimarFT* (lane 8). (C) Plasmid pFTNAT containing the nourseothricin resistance gene used for complementation of *HimarFT* mutant strains. (D) Western blot analysis of cell lysates using a mouse monoclonal anti-*F. tularensis* LPS antibody. The strains analyzed include LVS with pFTNAT (lane 1); LVS *wbtA1*::*HimarFT* alone (lane 2), with pFTNAT (lane 3), or with pFTNAT-$wbtA_{LVS}$ (lane 4); LVS *wbtA2*::*HimarFT* alone (lane 5), with pFTNAT (lane 6), or with pFTNAT-$wbtA_{LVS}$ (lane 7); and LVS *wbtM1*::*HimarFT* alone (lane 8), with pFTNAT (lane 9), or with pFTNAT-$wbtM_{LVS}$ (lane 10).

Fragments that were the correct size were obtained in PCR and RT-PCR controls with *F. tularensis* LVS genomic DNA, verifying that there was primer-mediated amplification of the correct region (Fig. 6B). Products were not detectable when template DNA was not included or in PCRs utilizing DNase-treated RNA isolated from wild-type or mutant strains, indicating that the preparations of RNA were not contaminated with genomic DNA (Fig. 6B). RT-PCRs with RNA isolated from LVS, LVS *wbtA1*::*HimarFT*, and *wbtA2*::*HimarFT* each demonstrated that there was a message containing *wbtD* on a fragment whose size was similar to that of the genomic DNA control (Fig. 6B). Similarly, a product was detected for all three strains when *wbtC* was the target sequence (data not shown). The amounts of *wbtC* and *wbtD* cDNAs appeared to be reduced in strains containing an upstream *HimarFT* insertion. These data suggest that *HimarFT* insertion is partially polar.

To complement *HimarFT* mutants, we constructed a new shuttle vector containing a nourseothricin resistance marker, pFTNAT (Fig. 6C). Nourseothricin is an antibiotic that inhibits a broad spectrum of organisms and is postulated to inhibit protein synthesis by induction of miscoding events (26). It is an

attractive marker for *Francisella* research as it is not used in human or veterinary medicine and has not been shown to display cross-resistance (42). Genomic fragments containing the genes and their predicted promoter regions for complementation were cloned into pFTNAT and transformed into the appropriate *HimarFT* mutant strains.

Complementation of mutants with insertions in either the *wbt* region or FTL_0706 was assessed both for O-antigen content and for cytopathogenicity in macrophages. O-antigen expression and cytopathogenicity were restored to *F. tularensis* LVS *wbtM*::*HimarFT* with pFTNAT-$wbtM_{LVS}$ in *trans* (Fig. 6D and data not shown). However, complementation of LVS *wbtA1*::*HimarFT* was not detected using a similar cloning strategy (pFTNAT-$wbtA_{LVS}$) (Fig. 6D). Partial restoration of O-antigen expression occurred when LVS *wbtA2*::*HimarFT* was transformed with pFTNAT-$wbtA_{LVS}$ (Fig. 6D), but this strain still displayed reduced cytopathogenicity compared to LVS (data not shown). The presence of plasmid pFTNAT did not alter the strain phenotypes. The lack of complementation or partial complementation is consistent with results from RT-PCR analyses and suggests that the orientation of *HimarFT* influences the expression of adjacent genes. These data also support an operon organization for the *wbt* region.

F. tularensis LVS FTL_0706-1::*HimarFT* and FTL_0706-2::*HimarFT* mutants were complemented in *trans* using pFTNAT-FTL_0706 (Fig. 7A). FTL_0706 does not appear to be part of an operon based on the current annotation of the LVS genome. FTL_0706 provided in *trans* restored the O-antigen ladder in both FTL_0706::*HimarFT* mutant strains (Fig. 7B). Cytopathogenicity was restored in LVS FTL_0706-1::*HimarFT* and FTL_0706-2::*HimarFT* with pFTNAT-FTL_0706, resulting in loss of the macrophage monolayer, similar to the parental phenotype (Fig. 7C).

Mutagenesis of *F. tularensis* Schu S4. FTL_0706 and FTT1238c are highly conserved hypothetical genes having variation in only two nucleotides in *F. tularensis* LVS and Schu S4, respectively (Fig. 8A). Therefore, we reasoned that introduction of the rescued plasmid carrying FTL_0706::*HimarFT* could be used to disrupt FTT1238c in Schu S4 (2, 3, 27, 36, 45). Electroporation of the nonreplicative plasmid into Schu S4 resulted in recovery of several Km^r clones, one of which was defective for the synthesis of O antigen like LVS FTL_0706-1::*HimarFT*. Other clones exhibited a parental O-antigen phenotype and were confirmed to be merodiploids by Southern blotting (Fig. 8B and C). Moreover, nucleotide sequence analysis of the Schu S4 mutants demonstrated that the first of two variable nucleotide differences in the locus was characteristic of LVS.

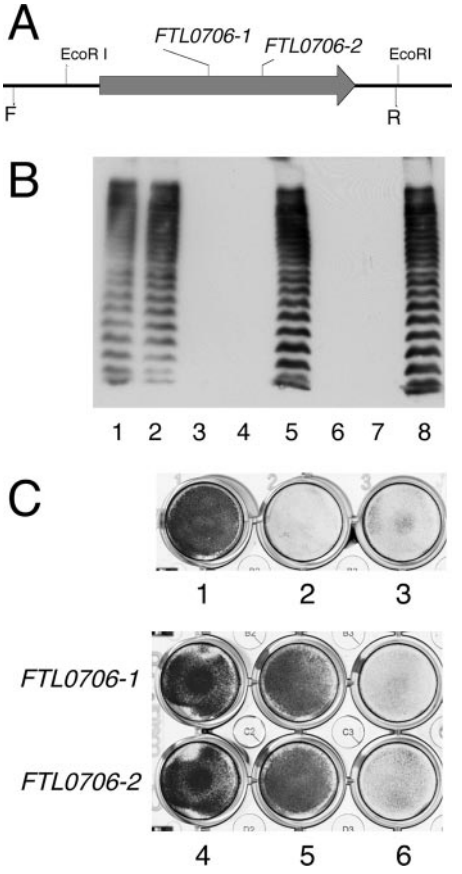

FIG. 7. Complementation of *F. tularensis* LVS FTL_0706::*HimarFT* mutant strains in *trans* using pFTNAT-FTL_0706. (A) Two mutants containing *HimarFT* insertions within FTL_0706 in opposite orientations were assessed for complementation (locations are indicated by the gene designation and candidate number). LVS FTL_0706-1::*HimarFT* contains the *groEL* promoter (p*gro*) in the same orientation as FTL_0706. F and R indicate the DNA fragment amplified from the genome, and the EcoRI sites indicate the fragment used for complementation. (B) Western blot analysis of cell lysates from LVS and LVS FTL_0706::*HimarFT* strains using a mouse monoclonal anti-*F. tularensis* LPS antibody. The strains analyzed include LVS without (lane 1) or with (lane 2) pFTNAT; LVS FTL_0706-1::*HimarFT* alone (lane 3), with pFTNAT (lane 4), and with pFTNAT-FTL_0706 (lane 5); and FTL_0706-2::*HimarFT* alone (lane 6), with pFTNAT (lane 7), and with pFTNAT-FTL_0706 (lane 8). (C) Cytopathic analysis with J774A.1 macrophages using crystal violet staining 2 days after infection at an MOI of 100. The retention of the monolayer after infection is compared to the uninfected control (well 1). Wells 2 and 3 contained wild-type LVS without and with pFTNAT. Wells 4 to 6 contained the *F. tularensis* LVS FTL_0706::*HimarFT* mutant candidates alone (wells 4), with pFTNAT (wells 5), and with pFTNAT-FTL_0706 (wells 6).

DISCUSSION

To gain a more comprehensive understanding of the gene products required for *F. tularensis* intracellular replication, a transposon-based mutagenesis strategy coupled with a simple high-throughput screen with macrophages was utilized. Several *HimarFT* mutants recovered after our screens contained insertions in previously identified genes important for macrophage growth, including *clpB*, *dsbB*, *capBC*, *aspC2*, and *wbtA* (28, 55, 58, 67, 69, 70, 76). However, some genes whose products are associated with virulence, including those located in the FPI, were not identified in our screen as strongly attenuated (2, 28, 44, 53, 55, 56, 69). The absence of some previously identified virulence factors in our pool could have been due to the growth and replication conditions used, the stringency of the screen, or the inability to rescue all of the clones with the highest potential of encoding critical functions for macrophage growth. Lastly, the results indicate that our library may not saturate the genome, although isolation of multiple *HimarFT* strains with mutations in the same genes suggests that good coverage was obtained.

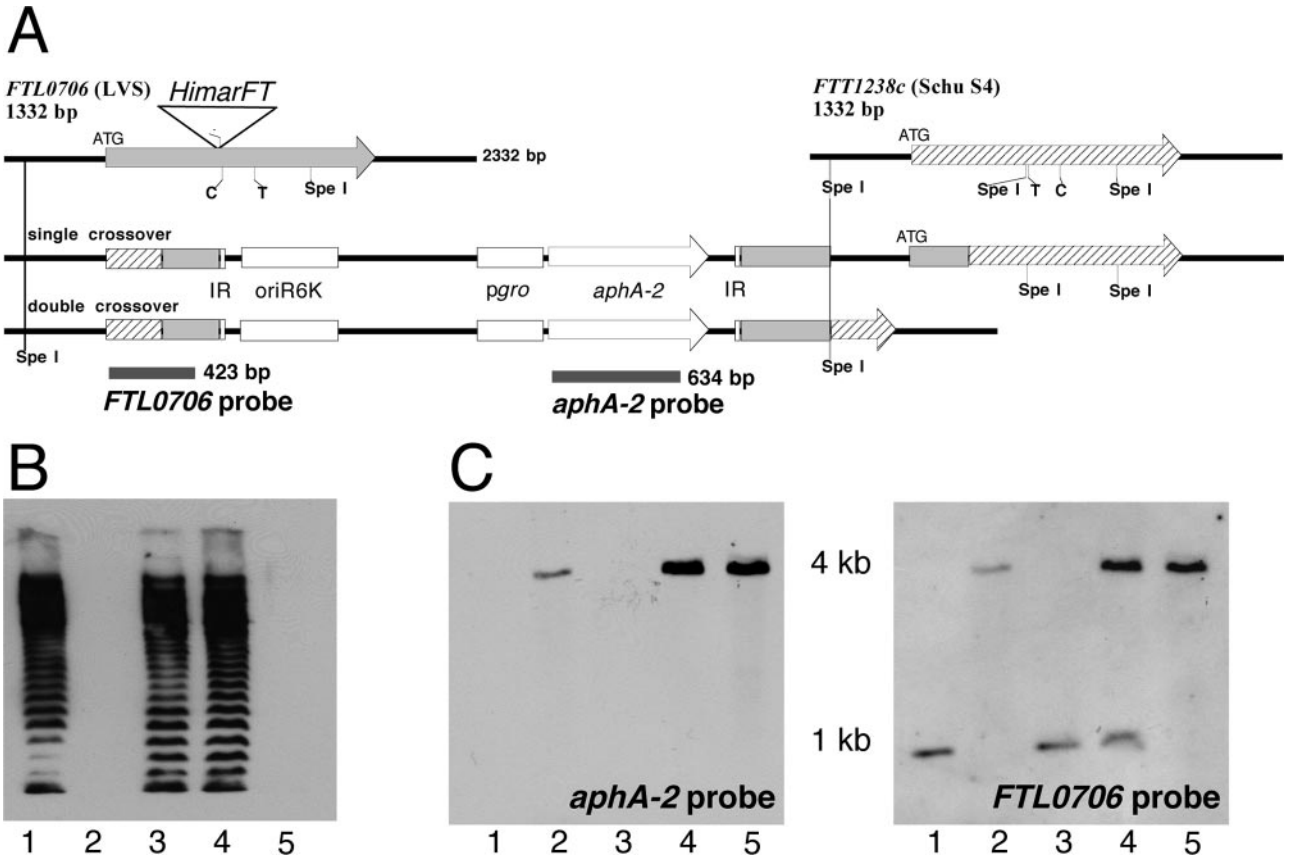

FIG. 8. Analysis of *HimarFT* insertions with mutations in FTL_0706 and FTT1238c for *F. tularensis* LVS and Schu S4, respectively. (A) LVS and Schu S4 wild-type loci are indicated by gray and striped arrows, respectively. *HimarFT* insertion into FTL_0706 in LVS resulted in the loss of an SpeI site present in the parental chromosomal locus. The sequence for this locus in LVS and Schu S4 is highly conserved, with variation in only two nucleotides, as shown. Introduction of a circularized SpeI fragment containing the *HimarFT* insertion from LVS FTL_0706-1::*HimarFT* into Schu S4 promoted homologous recombination resulting in either a single- or double-crossover event as indicated. (B) Western blot analysis of the LVS and Schu S4 strains with a mouse monoclonal anti-*F. tularensis* LPS antibody demonstrated the presence or absence of the LPS ladder. The strains analyzed were LVS (lane 1), LVS FTL_0706-1::*HimarFT* (lane 2), Schu S4 (lane 3), Schu S4 FTT1238c::*HimarFT* merodiploid (lane 4), and Schu S4 FTT1238c::*HimarFT* (lane 5). (C) Southern blot analysis to assess the presence of both *HimarFT* and FTL_0706 in the represented strains. SpeI-digested genomic DNA was probed with digoxigenin-labeled fragments of *aphA-2* (4-kb signal) or FTL_0706 (with and without *HimarFT* insertion; 4- and 1-kb signals, respectively). The lane contents are the same as those described above for panel B.

The FPI has potential roles in secretion, phagosome biogenesis, and subsequent escape into the cytosol or as an effector or cofactor element involved in promoting an optimal intracellular niche (14, 35, 50, 61, 62). It is duplicated in *F. tularensis* LVS, making it unlikely that isolates with mutations within this locus would have a strongly attenuated phenotype. *HimarFT* mutants in group C, demonstrating light retention of the crystal violet stain after stage 2 screening, were also subjected to nucleotide sequence analysis (data not shown). This analysis yielded insertions in the FPI *iglB*, *iglC*, and *iglD* loci, suggesting that deletion of one copy of these genes may result in a partial loss of function in *F. tularensis* LVS. This is consistent with a slight reduction in the BALB/c mouse lung survival of an EZ::TN-derived *iglC* LVS mutant (67). Interestingly, allelic replacement of both *iglC* loci in LVS was required to inhibit growth in J774A.1 and mouse peritoneal macrophages (27). These data indicate that the copy number of the FPI members is important for virulence.

As expected, *HimarFT* mutagenesis in *F. tularensis* LVS yielded a variety of genes encoding functions predicted to be important for intracellular survival and replication, as well as a number of hypothetical open reading frames. The identification of virulence determinants can be influenced by growth conditions, the properties of the transposon element, the *F. tularensis* subspecies used, or the choice of screening criteria. Despite these differences, similar functional groups of genes have been identified utilizing a variety of strategies in *Francisella* (28, 55, 67, 69, 76). Replication, translation, and protein modification and/or turnover genes were represented, including genes encoding proteins with predicted functions in disulfide bond formation, glutathione metabolism, or proteolytic degradation. Genes involved in metabolism and transport were prevalent, consistent with intracellular persistence requiring a variety of substrates, including amino acids, iron, and extracellular proteins (4, 16, 30, 37, 53, 56, 68). We speculate that the differences in stresses induced during growth in broth or on plates compared with intracellular growth may account for the identification of this class of genes. One candidate with a potential role in protein folding/stability or transport (FTL_1096) is located downstream of a predicted macrophage infectivity potentiator.

Protein processing, metabolic, and transport-deficient mutants have the potential to be the basis for a new vaccine since they can infect and transmit their surface antigens but are likely limited in promoting overt disease. Surprisingly, although purines are clearly essential for intracellular growth of *Francisella* (28, 53, 55, 56, 67, 69, 76), mutants with insertions in this pathway were not recovered from our library. This was likely due to culture conditions in which medium lacking protease peptone was used in the selection step for transposon insertions (53).

A variety of surface structures, including LPS (13, 58, 63, 70), capsule (60, 67), type IV pilin (20, 24, 30), and outer membrane channels or proteins (32, 52), are implicated in *Francisella* virulence through potential roles in adherence, uptake, or phagosomal escape. In this study, several insertions within genes encoding capsule, LPS, and transporters were identified. *F. tularensis* LPS displays low toxicity compared to other gram-negative bacteria, and the structures of the O antigen and its corresponding gene cluster (*wbt* locus) in *F. tularensis* LVS and Schu S4 are identical but distinctly different from that in *F. tularensis* subsp. *novicida* (44). This is consistent with variation in detection with anti-LPS antibodies and induced immunity and/or cross-protection (22, 70, 75). O-antigen expression is defective when *HimarFT* insertions map to *wbtA*, a result that is similar to results previously reported by other groups (13, 58, 63). *HimarFT* mutants with mutations in *wbtM* and *wbtC* also displayed an O-antigen-defective phenotype not previously reported. Although *wbtA* and *wbtM* both encode a predicted dTDP-glucose 4,6-dehydratase, the gene sequences and the protein domains are quite different, suggesting that there are distinct roles for each protein. Interestingly, mutation of the *wbtA* and *wbtDEF* loci in several subspecies results in O-antigen loss but is accompanied by variable effects on intracellular survival (13, 58, 63, 70). These differences were also observed in our study. LVS FTL_0706::*HimarFT* appears to be similar to mutant SC92 recovered for *F. tularensis* subsp. *novicida* (13), but the O-antigen and intracellular growth phenotypes were not congruent. The LVS FTL_0706::*HimarFT* strain had a complete loss of O antigen and a 1,000-fold reduction in intracellular replication. In contrast, a partial loss of O antigen and a 10-fold decrease in replication occurred in SC92. The variation in O antigen is due to either distinct roles in biosynthesis in different subspecies or variable recognition by the antibodies used. FTL_0706 is located near another locus predicted to be involved in LPS biosynthesis but does not appear to be part of an operon.

HimarFT mutants with insertions in hypothetical genes displayed several distinct phenotypes related to intracellular replication and cytotoxicity. There was no significant difference between *F. tularensis* LVS and the strains bearing *HimarFT* insertions in terms of the ability to enter J774A.1 macrophages. Five of the seven *HimarFT* mutants exhibited significantly reduced replication and cytotoxicity, consistent with their attenuation in mice. In general, the intracellular growth of these strains was variably hampered, and the strains exhibited reduced levels of cytotoxicity, similar to the pattern exhibited by LVS Δ*purMCD*. The yield of viable bacteria from macrophages at 24 h for mutants with insertions in FTL_0886, FTL_1414, and FTL_0439 was significantly reduced compared to that of the parental strain, but these cultures contained approximately 100-fold more bacteria than cultures of the avirulent LVS Δ*purMCD* mutant with a similar level of cytotoxicity. This suggests that cytotoxicity may be induced by specific bacterial activities perhaps encoded by FTL_0886, FTL_1414, or FTL_0439. Despite displaying attenuation in the mouse model of infection, mutation of FTL_1096 resulted in no significant change in cytotoxicity, and insertion in FTL_0544 resulted in no significant changes in either cytotoxicity or replication compared to the wild type. This phenomenon has been observed in several EZ::TN-derived transposon mutants of *F. tularensis* subsp. *novicida* (76). The use of several model systems and *Francisella* strains to dissect gene function should allow reconciliation between in vitro and in vivo phenotypes. For example, there were reported differences in attenuation among different isolates of LVS or Schu S4 (29, 74), when different in vitro models (diverse macrophage or hepatic cell lines) were assessed (55, 69), or when in vitro and in vivo results were compared (20, 25, 69).

Recent studies indicate that inactivation of FTT0918 in *F. tularensis* Schu S4 results in subsequent loss of a 58-kDa protein and attenuation in vivo (72). FTT0918/FTT0919 represents a new protein family with predicted signal peptides and/or coiled-coil domains commonly associated with membranes and/or secretion (32, 35, 72). Interestingly, the N-terminal domain of FTT0918 and the C-terminal domain of FTT0919 form a single hybrid protein in *F. tularensis* type A strain FSC043 and type B strain LVS (FTL_0439). It has been suggested that part of the observed attenuation of LVS could be due to the deletion and fusion events that altered the FTT0918/FTT0919 locus (54, 59, 72). In this study, inactivation of FTL_0439 in *F. tularensis* LVS resulted in attenuation in vitro and in vivo. Thus, despite the hybrid nature of FTL_0439, it appears to maintain an important role in the virulence of LVS and is not likely to be the cause of its attenuation.

Polarity is an important consideration in determining whether a specific transposon insertion results in the observed phenotype. To address whether *HimarFT* is polar, RT-PCR and complementation analyses were performed with strains containing insertions mapping to genes that are or are not postulated to be part of a larger operon structure. Semiquantitative RT-PCRs of the *wbt* operon demonstrated that when target regions downstream of *HimarFT* were assessed, there was a reduction in the amount of cDNA detected. The data indicate that *HimarFT* insertion affects distal gene expression. Previous complementation experiments have utilized a highly active promoter, such as *groEL*, to ensure gene expression in the absence of a native promoter. However, alteration in the level of expression of the gene in *trans* can be detrimental (14, 38, 61, 67). Since the native promoter was used for complementation in our studies, the partial restoration of O antigen in *F. tularensis* LVS *wbtA2*::*HimarFT* pFTNAT-$wbtA_{LVS}$ was not due to overexpression of the gene in *trans*. In fact, a similar partial restoration of O antigen was observed in an LVS *Himar1*-based *wbtA* mutant when *wbtA* was driven by the *groEL* promoter in *trans* (63). Based on our RT-PCR and complementation patterns, we concluded that the *groEL* promoter from *HimarFT* transcribes into flanking gene regions. In *trans* complementation analysis verified that the noncytopathic phenotypes of mutants with insertions in both *wbtM* and FTL_0706 were due to the *HimarFT* insertion. Neither of these genes appears to be part of an operon.

In summary, after a *HimarFT* insertion library was screened for candidates deficient in cytopathogenicity in J774A.1 macrophages, 26 genes were identified as virulence determinants in *Francisella*. Several candidates have been reported in previous genetic analyses, validating our screening process, while others were recognized for the first time as potential virulence factors. Along with genes involved in transport, metabolism, protein stability/turnover, and surface components, seven mutants with insertions in hypothetical genes were recovered. All of these mutants were attenuated in a BALB/c mouse model of infection, suggesting that there is a direct correlation between in vitro and in vivo replication. Complementation analysis of selected strains confirmed that the phenotype observed was due to the gene in which *HimarFT* inserted. It also provided evidence for potential polar effects that can affect the expression of genes adjacent to *HimarFT* insertions. Additional studies of our candidate genes and the design of alternative screens should further define components important for the intracellular lifestyle of *Francisella*, provide insight into the mechanisms involved in infection, and facilitate the development of therapeutics and/or a defined vaccine effective for the identification and control of this invasive pathogen.

ACKNOWLEDGMENTS

This work was sponsored by the NIH/NIAID Regional Center of Excellence for Biodefense and Emerging Infectious Diseases Research (RCE) Program, the Center for Biopreparedness and Infectious Disease at the Medical College of Wisconsin, and NIH funds (grant AI 063441 to D.W.F. and T.C.Z.). T.M.M. and C.W.D. were supported by Great Lakes Regional Center of Excellence career development fellowships CDP9 and CDP19.

We thank Marc A. Benson for his assistance with compiling the *F. tularensis* LVS *HimarFT* library. Travis McCarthy kindly assisted in generating the RT-PCR results.

REFERENCES

1. **Altschul, S. F., W. Gish, W. Miller, E. W. Myers, and D. J. Lipman.** 1990. Basic local alignment search tool. J. Mol. Biol. **215:**403–410.
2. **Anthony, L. S., S. C. Cowley, K. E. Mdluli, and F. E. Nano.** 1994. Isolation of a *Francisella tularensis* mutant that is sensitive to serum and oxidative killing and is avirulent in mice: correlation with the loss of MinD homologue expression. FEMS Microbiol. Lett. **124:**157–165.
3. **Anthony, L. S. D., M. Z. Gu, S. C. Cowley, W. W. S. Leung, and F. E. Nano.** 1991. Transformation and allelic replacement in *Francisella* spp. J. Gen. Microbiol. **137:**2697–2703.
4. **Atkins, H. S., E. Dassa, N. J. Walker, K. F. Griffin, D. N. Harland, R. R. Taylor, M. L. Duffield, and R. W. Titball.** 2006. The identification and evaluation of ATP binding cassette systems in the intracellular bacterium *Francisella tularensis*. Res. Microbiol. **157:**593–604.
5. **Bendtsen, J. D., H. Nielsen, G. von Heijne, and S. Brunak.** 2004. Improved prediction of signal peptides: SignalP 3.0. J. Mol. Biol. **340:**783–795.
6. **Bina, X. R., C. Wang, M. A. Miller, and J. E. Bina.** 2006. The Bla2 β-lactamase from the live-vaccine strain of *Francisella tularensis* encodes a functional protein that is only active against penicillin-class β-lactam antibiotics. Arch. Microbiol. **186:**219–228.
7. **Broekhuijsen, M., P. Larsson, A. Johansson, M. Byström, U. Eriksson, E. Larsson, R. G. Prior, A. Sjöstedt, R. W. Titball, and M. Forsman.** 2003. Genome-wide DNA microarray analysis of *Francisella tularensis* strains demonstrates genetic conservation within the species but identifies regions that are unique to the highly virulent *F. tularensis* subsp. *tularensis.* J. Clin. Microbiol. **41:**2924–2931.
8. **Burke, D. S.** 1977. Immunization against tularemia: analysis of the effectiveness of live *Francisella tularensis* vaccine in prevention of laboratory-acquired tularemia. J. Infect. Dis. **135:**55–60.
9. **Camilli, A., D. A. Portnoy, and P. Youngman.** 1990. Insertional mutagenesis of *Listeria monocytogenes* with a novel Tn*917* derivative that allows direct cloning of DNA flanking transposon insertions. J. Bacteriol. **172:**3738–3744.
10. **Chamberlain, R. E.** 1965. Evaluation of live tularemia vaccine prepared in a chemically defined medium. Appl. Microbiol. **13:**232–235.
11. **Checroun, C., T. D. Wehrly, E. R. Fischer, S. F. Hayes, and J. Celli.** 2006. Autophagy-mediated reentry of *Francisella tularensis* into the endocytic compartment after cytoplasmic replication. Proc. Natl. Acad. Sci. USA **103:** 14578–14583.
12. **Chen, W., H. Shen, A. Webb, R. KuoLee, and J. W. Conlan.** 2003. Tularemia in BALB/c and C57BL/6 mice vaccinated with *Francisella tularensis* LVS and challenged intradermally, or by aerosol with virulent isolates of the pathogen: protection varies depending on pathogen virulence, route of exposure, and host genetic background. Vaccine **21:**3690–3700.
13. **Cowley, S. C., C. J. Gray, and F. E. Nano.** 2000. Isolation and characterization of *Francisella novicida* mutants defective in lipopolysaccharide biosynthesis. FEMS Microbiol. Lett. **182:**63–67.
14. **de Bruin, O. M., J. S. Ludu, and F. E. Nano.** 2007. The *Francisella* pathogenicity island protein IglA localizes to the bacterial cytoplasm and is needed for intracellular growth. BMC Microbiol. **7:**1.
15. **Dempsey, M. P., J. Nietfeldt, J. Ravel, S. Hinrichs, R. Crawford, and A. K. Benson.** 2006. Paired-end sequence mapping detects extensive genomic rearrangement and translocation divergence of *Francisella tularensis* subsp. *tularensis* and *Fracisella tularensis* subsp. *holarctica* populations. J. Bacteriol. **188:**5904–5914.
16. **Deng, K., R. Blick, W. Liu, and E. J. Hansen.** 2006. Identification of *Francisella tularensis* genes affected by iron limitation. Infect. Immun. **74:**4224–4236.
17. **Eigelsbach, H. T., W. Braun, and R. D. Herring.** 1951. Studies on the variation of *Bacterium tularense*. J. Bacteriol. **61:**557–569.
18. **Eigelsbach, H. T., and C. M. Downs.** 1961. Prophylactic effectiveness of live and killed tularemia vaccines. I. Production of vaccine and evaluation in the white mouse and guinea pig. J. Immunol. **87:**415–425.
19. **Ellis, J., P. C. Oyston, M. Green, and R. W. Titball.** 2002. Tularemia. Clin. Microbiol. Rev. **15:**631–646.
20. **Forslund, A. L., K. Kuoppa, K. Svensson, E. Salomonsson, A. Johansson, M. Bystrom, P. C. F. Oyston, S. L. Michell, R. W. Titball, L. Noppa, E. Frithz-Lindsten, M. Forsman, and A. Forsberg.** 2006. Direct repeat-mediated deletion of a type IV pilin gene results in major virulence attenuation of *Francisella tularensis*. Mol. Microbiol. **59:**1818–1830.
21. **Fortier, A. H., M. V. Slayter, R. Ziemba, M. S. Meltzer, and C. A. Nacy.** 1991. Live vaccine strain of *Francisella tularensis*: infection and immunity in mice. Infect. Immun. **59:**2922–2928.
22. **Fulop, M. J., T. Webber, R. J. Manchee, and D. C. Kelly.** 1991. Production and characterization of monoclonal antibodies directed against the lipopolysaccharide of *Francisella tularensis*. J. Clin. Microbiol. **29:**1407–1412.
23. **Gallagher, L. A., E. Ramage, M. A. Jacobs, R. Kaul, M. Brittnacher, and C. Manoil.** 2007. A comprehensive transposon mutant library of *Francisella novicida*, a bioweapon surrogate. Proc. Natl. Acad. Sci. USA **104:**1009–1014.
24. **Gil, H., J. L. Benach, and D. G. Thanassi.** 2004. Presence of pili on the surface of *Francisella tularensis*. Infect. Immun. **72:**3042–3047.
25. **Gil, H., G. J. Platz, C. A. Forestal, M. Monfett, C. S. Bakshi, T. J. Sellati, M. B. Furie, J. L. Benach, and D. G. Thanassi.** 2006. Deletion of TolC orthologs in *Francisella tularensis* identifies roles in multidrug resistance and virulence. Proc. Natl. Acad. Sci. USA **103:**12897–12902.
26. **Goldstein, A. L., and J. H. McCusker.** 1999. Three new dominant drug resistance cassettes for gene disruption in *Saccharomyces cerevisiae*. Yeast **15:**1541–1553.
27. **Golovliov, I., A. Sjöstedt, A. N. Mokrievich, and V. M. Pavlov.** 2003. A method for allelic replacement in *Francisella tularensis*. FEMS Microbiol. Lett. **222:**273–280.
28. **Gray, C. G., S. C. Cowley, K. K. Cheung, and F. E. Nano.** 2002. The identification of five genetic loci of *Francisella novicida* associated with intracellular growth. FEMS Microbiol. Lett. **215:**53–56.
29. **Green, M., G. Choules, D. Rogers, and R. W. Titball.** 2005. Efficacy of the live attenuated *Francisella tularensis* vaccine (LVS) in a murine model of disease. Vaccine **23:**2680–2686.
30. **Hager, A. J., D. L. Bolton, M. R. Pelletier, M. J. Brittnacher, L. A. Gallagher, R. Kaul, S. J. Skerrett, S. I. Miller, and T. Guina.** 2006. Type IV pili-mediated secretion modulates *Francisella* virulence. Mol. Microbiol. **62:**227–237.
31. **Henikoff, S., J. G. Henikoff, W. J. Alford, and S. Pietrokovski.** 1995. Automated construction and graphical presentation of protein blocks from unaligned sequences. Gene **163:**GC17–GC26.
32. **Huntley, J. F., P. G. Conley, K. E. Hagman, and M. V. Norgard.** 2007. Characterization of *Francisella tularensis* outer membrane proteins. J. Bacteriol. **189:**561–574.
33. **Kawula, T. H., J. D. Hall, J. R. Fuller, and R. R. Craven.** 2004. Use of transposon-transposase complexes to create stable insertion mutant strains of *Francisella tularensis* LVS. Appl. Environ. Microbiol. **70:**6901–6904.
34. **Larson, C. L., W. Wicht, and W. L. Jellison.** 1955. A new organism resembling *P. tularensis* isolated from water. Public Health Rep. **70:**253–258.
35. **Larsson, P., P. C. F. Oyston, P. Chain, M. C. Chu, M. Duffield, H.-H. Fuxelius, E. Garcia, G. Halltorp, D. Johansson, K. E. Isherwood, P. D. Karp, E. Larsson, Y. Liu, S. Michell, J. Prior, R. Prior, S. Malfatti, A. Sjostedt, K. Svensson, N. Thompson, L. Vergez, J. K. Wagg, B. W. Wren, L. Lindler, S. G. E. Andersson, M. Forsman, and R. W. Titball.** 2005. The complete genome sequence of *Francisella tularensis*, the causative agent of tularemia. Nat. Genet. **37:**153–159.

36. **Lauriano, C. M., J. R. Barker, F. E. Nano, B. P. Arulanandam, and K. E. Klose.** 2003. Allelic exchange in *Francisella tularensis* using PCR products. FEMS Microbiol. Lett. **229:**195–202.
37. **Lee, B.-Y., M. A. Horwitz, and D. L. Clemens.** 2006. Identification, recombinant expression, immunolocalization in macrophages, and T-cell responsiveness of the major extracellular proteins of *Francisella tularensis*. Infect. Immun. **74:**4002–4013.
38. **Lindgren, H., I. Golovliov, V. Baranov, R. K. Ernst, M. Telepnev, and A. Sjöstedt.** 2004. Factors affecting the escape of *Francisella tularensis* from the phagolysosome. J. Med. Microbiol. **53:**953–958.
39. **Lopez, M. C., N. S. Duckett, S. D. Baron, and D. W. Metzger.** 2004. Early activation of NK cells after lung infection with the intracellular bacterium, Francisella tularensis LVS. Cell. Immunol. **232:**75–85.
40. **LoVullo, E. D., L. A. Sherrill, L. L. Perez, and M. S. J. Pavelka.** 2006. Genetic tools for highly pathogenic *Francisella tularensis* subsp. *tularensis.* Microbiol. **152:**3425–3435.
41. **Maier, T. M., A. Havig, M. Casey, F. E. Nano, D. W. Frank, and T. C. Zahrt.** 2004. Construction and characterization of a highly efficient *Francisella* shuttle plasmid. Appl. Environ. Microbiol. **70:**7511–7519.
42. **Maier, T. M., R. Pechous, M. Casey, T. C. Zahrt, and D. W. Frank.** 2006. In vivo *Himar1*-based transposon mutagenesis of *Francisella tularensis*. Appl. Environ. Microbiol. **72:**1878–1885.
43. **Maltsev, N., E. Glass, D. Sulakhe, A. Rodriguez, M. Syed, T. Bompada, and Y. Zhang.** 2006. PUMA2—grid-based high-throughput analysis of genomes and metabolic pathways. Nucleic Acids Res. **34:**D369–D372.
44. **McLendon, M. K., M. A. Apicella, and L.-A. H. Allen.** 2006. *Francisella tularensis*: taxonomy, genetics, and immunopathogenesis of a potential agent of biowarfare. Annu. Rev. Microbiol. **60:**167–185.
45. **Mdluli, K. E., L. S. Anthony, G. S. Baron, M. K. McDonald, S. V. Myltseva, and F. E. Nano.** 1994. Serum-sensitive mutation of *Francisella novicida*: association with an ABC transporter gene. Microbiology **140:**3309–3318.
46. **Mohapatra, N. P., S. Soni, B. L. Bell, R. Warren, R. K. Ernst, A. Muszynski, R. W. Carlson, and J. S. Gunn.** 2007. Identification of an orphan response regulator required for *Francisella* virulence and transcription of pathogenicity island genes. Infect. Immun. **75:**3305–3314.
47. **Moller, S., M. D. R. Croning, and R. Apweiler.** 2001. Evaluation of methods for the prediction of membrane spanning regions. Bioinformatics **17:**646–653.
48. **Mulder, N. J., R. Apweiler, T. K. Attwood, A. Bairoch, D. Barrell, A. Bateman, D. Binns, M. Biswas, P. Bradley, P. Bork, P. Bucher, R. R. Copley, E. Courcelle, U. Das, R. Durbin, L. Falquet, W. Fleischmann, S. Griffiths-Jones, D. Haft, N. Harte, N. Hulo, D. Kahn, A. Kanapin, M. Krestyaninova, R. Lopez, I. Letunic, D. Lonsdale, V. Silventoinen, S. E. Orchard, M. Pagni, D. Peyruc, C. P. Ponting, J. D. Selengut, F. Servant, C. J. Sigrist, R. Vaughan, and E. M. Zdobnov.** 2003. The InterPro Database, 2003 brings increased coverage and new features. Nucleic Acids Res. **31:**315–318.
49. **Nallapareddy, S., K. Singh, and B. Murray.** 2006. Construction of improved temperature-sensitive and mobilizable vectors and their use for constructing mutations in the adhesion-encoding *acm* gene of poorly transformable clinical *Enterococcus faecium* strains. Appl. Environ. Microbiol. **72:**334–345.
50. **Nano, F. E., N. Zhang, S. C. Cowley, K. E. Klose, K. K. M. Cheung, M. J. Roberts, J. S. Ludu, G. W. Letendre, A. I. Meierovics, G. Stephens, and K. L. Elkins.** 2004. A *Francisella tularensis* pathogenicity island required for intramacrophage growth. J. Bacteriol. **186:**6430–6436.
51. **Oyston, P. C. F., A. Sjostedt, and R. W. Titball.** 2004. Tularaemia: bioterrorism defence renews interest in *Francisella tularensis*. Nat. Rev. **2:**967–978.
52. **Pavkova, I., M. Hubálek, J. Zechovska, J. Lenco, and J. Stulik.** 2005. *Francisella tularensis* live vaccine strain: proteomic analysis of membrane proteins enriched fraction. Proteomics **5:**2460–2467.
53. **Pechous, R., J. Celli, R. Penoske, S. F. Hayes, D. W. Frank, and T. C. Zahrt.** 2006. Construction and characterization of an attenuated purine auxotroph in a *Francisella tularensis* live vaccine strain. Infect. Immun. **74:**4452–4461.
54. **Petrosino, J. F., Q. Xiang, S. E. Karpathy, H. Jiang, S. Yerrapragada, Y. Liu, J. Gioia, L. Hemphill, A. Gonzalez, T. M. Raghavan, A. Uzman, G. E. Fox, S. Highlander, M. Reichard, R. J. Morton, K. D. Clinkenbeard, and G. M. Weinstock.** 2006. Chromosome rearrangement and diversification of *Francisella tularensis* revealed by the type B (OSU18) genome sequence. J. Bacteriol. **188:**6977–6985.
55. **Qin, A., and B. J. Mann.** 2006. Identification of transposon insertion mutants of *Francisella tularensis tularensis* strain Schu S4 deficient in intracellular replication in the hepatic cell line HepG2. BMC Microbiol. **6:**69.
56. **Quarry, J. E., K. E. Isherwood, S. L. Michell, H. Diaper, R. W. Titball, and P. C. F. Oyston.** 2007. A *Francisella tularensis* subspecies *novicida purF* mutant, but not a *purA* mutant, induces protective immunity to tularemia in mice. Vaccine **25:**2011–2018.
57. **Rasko, D. A., C. D. Esteban, and V. Sperandio.** 2007. Development of novel plasmid vectors and a promoter trap system in *Francisella tularensis* compatible with the pFNL10 based plasmids. Plasmid **58:**159–166.
58. **Raynaud, C., K. L. Meiborn, M. A. Lety, I. Dubail, T. Candela, E. Frapy, and A. Charbit.** 2007. Role of the *wbtA* locus of *Fransicella tularensis* in lipopolysaccharide O-antigen biogenesis and pathogenicity. Infect. Immun. **75:**536–541.
59. **Rohmer, L., M. Brittnacher, K. Svensson, D. Buckley, E. Haugen, Y. Zhou, J. Chang, R. Levy, H. Hayden, M. Forsman, M. Olson, A. Johansson, R. Kaul, and S. I. Miller.** 2006. Potential source of *Francisella tularensis* live vaccine strain attenuation determined by genome comparison. Infect. Immun. **74:**6895–6906.
60. **Sandström, G., S. Löfgren, and A. Tärnvik.** 1988. A capsule-deficient mutant of *Francisella tularensis* LVS exhibits enhanced sensitivity to killing by serum but diminished sensitivity to killing by polymorphonuclear leukocytes. Infect. Immun. **56:**1194–1202.
61. **Santic, M., M. Molmeret, J. R. Barker, K. E. Klose, A. Dekanic, M. Doric, and Y. Abu Kwaik.** 21 May 2007, posting date. A *Francisella tularensis* pathogenicity island protein essential for bacterial proliferation within the host cytosol. Cell. Microbiol. doi:10.1111/j. 1462–5822.2007.00968.x. (Subsequently published, Cell. Microbiol. **9:**2391–2403, 2007.)
62. **Santic, M., M. Molmeret, K. E. Klose, S. Jones, and Y. Abu Kwaik.** 2005. The *Francisella tularensis* pathogenicity island protein IglC and its regulator MglA are essential for modulating phagosome biogenesis and subsequent bacterial escape into the cytoplasm. Cell. Microbiol. **7:**969–979.
63. **Sebastian, S., S. T. Dillon, J. G. Lynch, L. T. Blalock, E. Balon, K. T. Lee, L. E. Comstock, J. W. Conlan, E. J. Rubin, A. O. Tzianabos, and D. L. Kasper.** 2007. A defined O-antigen polysaccharide mutant of *Francisella tularensis* live vaccine strain has attenuated virulence while retaining its protective capacity. Infect. Immun. **75:**2591–2602.
64. **Shaw, K. J., P. N. Rather, R. S. Hare, and G. H. Miller.** 1993. Molecular genetics of aminoglycoside resistance genes and familial relationships of the aminoglycoside-modifying enzymes. Microbiol. Rev. **57:**138–163.
65. **Sjostedt, A.** 2006. Intracellular survival mechanisms of *Francisella tularensis*, a stealth pathogen. Microbes Infect. **8:**561–567.
66. **Sjöstedt, A.** 2003. Virulence determinants and protective antigens of *Francisella tularensis*. Curr. Opin. Microbiol. **6:**66–71.
67. **Su, J., J. Yang, D. Zhao, T. H. Kawula, J. A. Banas, and J. R. Zhang.** 2007. Genome-wide identification of *Francisella tularensis* virulence determinants. Infect. Immun. **75:**3089–3101.
68. **Sullivan, J., E. Jeffery, J. Shannon, and G. Ramakrishnan.** 2006. Characterization of the siderophore of *Francisella tularensis* and role of *fslA* in siderophore production. J. Bacteriol. **188:**3785–3795.
69. **Tempel, R., X. H. Lai, L. Crosa, B. Kozlowicz, and F. Heffron.** 2006. Attenuated *Francisella novicida* transposon mutants protect mice against wild-type challenge. Infect. Immun. **74:**5095–5105.
70. **Thomas, R. M., R. W. Titball, P. C. Oyston, K. Griffin, E. Waters, P. G. Hitchen, S. L. Michell, I. D. Grice, J. C. Wilson, and J. L. Prior.** 2007. The immunologically distinct O-antigens from *Francisella tularensis* subspecies *tularensis* and *Francisella novicida* are both virulence determinants and protective antigens. Infect. Immun. **75:**371–378.
71. **Titball, R. W., A. Johansson, and M. Forsman.** 2003. Will the enigma of *Francisella tularensis* virulence soon be solved? Trends Microbiol. **11:**118–123.
72. **Twine, S., M. Bystrom, W. Chen, M. Forsman, I. Golovliov, A. Johansson, J. Kelly, H. Lindgren, K. Svensson, C. Zingmark, W. Conlan, and A. Sjostedt.** 2005. A mutant of *Francisella tularensis* strain Schu S4 lacking the ability to express a 58-kilodalton protein is attenuated for virulence and is an effective live vaccine. Infect. Immun. **73:**8345–8352.
73. **Twine, S. M., N. C. Mykytezuk, M. D. Petit, H. Shen, A. Sjostedt, W. J. Colan, and J. F. Kelly.** 2006. In vivo proteomic analysis of the intracellular bacterial pathogen, Francisella tularensis isolated from mouse spleen. Biochem. Biophys. Res. Commun. **345:**1621–1633.
74. **Twine, S. M., H. Shen, J. F. Kelly, W. Chen, A. Sjostedt, and J. W. Conlan.** 2006. Virulence comparison in mice of distinct isolates of type A *Franicsella tularensis*. Microb. Pathog. **40:**133–138.
75. **Vinogradov, E., W. J. Conlan, J. S. Gunn, and M. B. Perry.** 2004. Characterization of the lipopolysaccharide O-antigen of *Francisella novicida* (U112). Carbohydr. Res. **339:**649–654.
76. **Weiss, D. S., A. Brotcke, T. Henry, J. J. Margolis, K. Chan, and D. M. Monack.** 2007. *In vivo* negative selection screen identifies genes required for *Francisella* virulence. Proc. Natl. Acad. Sci. USA **104:**6037–6042.

Editor: J. B. Bliska